Biometals (2010) 23:339–354
DOI 10.1007/s10534-010-9302-8

Zinc pyrithione induces cellular stress signaling and apoptosis in Hep-2 cervical tumor cells: the role of mitochondria and lysosomes

Emil Rudolf · Miroslav Červinka

Received: 4 November 2009 / Accepted: 2 February 2010 / Published online: 12 February 2010

Abstract Increased intracellular free zinc concentrations are associated with activation of several stress signaling pathways, specific organelle injury and final cell death. In the present work we examined the involvement of mitochondria and lysosomes and their crosstalk in free zinc-induced cell demise. We report that treatment of cervical tumor Hep-2 cells with zinc pyrithione leads to an early appearance of cytoplasmic zinc-specific foci with corresponding accumulation of zinc first in mitochondria and later in lysosomes. Concomitant with these changes, upregulation of expression of metallothionein II A gene as well as the increased abundance of its protein occurs. Moreover, zinc activates p53 and its dependent genes including Puma and Bax and they contribute to an observed loss of mitochondrial membrane potential and activation of apoptosis. Conversely, lysosomal membrane permeabilization and its promoted cleavage of Bid occurs in a delayed manner in treated cells and their effect on decrease of mitochondrial membrane potential is limited. The use of specific inhibitors as well as siRNA technology suggest a crucial role of MT-IIA in trafficking of free zinc into mitochondria or lysosomes and regulation of apoptotic or necrotic cell demise.

Keywords Zinc · Mitochondria · Lysosomes · Metallothionein · Apoptosis · Necrosis

E. Rudolf (✉) · M. Červinka
Department of Medical Biology and Genetics, Faculty of Medicine in Hradec Králové, Charles University in Prague, Šimkova 870, 500 01 Hradec Kralove I, Czech Republic
e-mail: rudolf@lfhk.cuni.cz

Introduction

Zinc (Zn) is a trace element which plays an important role in regulation of numerous cellular functions. Cells maintain optimal Zn stores required for cellular homeostasis by employing a set of complex mechanisms which ensure that most intracellular Zn remains in a bound form while free Zn is kept at minimum due to its high reactivity and potential cytotoxicity (Maret 2009). Using this strategy cells may tolerate even relatively high intracellular Zn concentrations which are currently estimated to be in a range of μM (Krezel and Maret 2006). Still, it is nowadays known that several processes including oxidant-induced cell injury or elevated local extracellular Zn concentrations may acutely increase intracellular free Zn levels resulting in cytotoxicity and cell death which is likely contributing to a number of pathologies such as neurodegenerative diseases or stroke (Sensi and Jeng 2004). On the other

hand, cytotoxicity of elevated intracellular free Zn levels in tumor cells is considered positive since it may limit tumor growth and ultimately may lead to its destruction, in particular in neoplasias characterized by impaired Zn homeostasis such as prostate cancer and breast cancer (Franklin and Costello 2007).

The exact mechanism whereby increased free Zn injures cells still remains unclear but available evidence suggests its pleiotropic nature in different cell types. Thus it has been reported that free Zn levels at pM to low nM range inhibit enzyme activity, deplete antioxidant systems, impair energy metabolism and induce oxidative stress (Dineley et al. 2003; Hogstrand et al. 1999; Maret et al. 1999; Provinciali et al. 2002; Ye et al. 2001). Moreover, free Zn may potentially interact with DNA, mitochondria or lysosomes and activate cell death signaling cascades (Lee et al. 2009; Sensi et al. 2003a, b). The cell death-inducing mechanism(s) of free Zn appear to be cell type dependent and include both extrinsic and intrinsic apoptotic pathways; however, with a significant contribution of various signaling molecules in individual cell populations. Thus in prostate cancer cells PC-3, Zn was shown to act directly on mitochondria via increasing mitochondrial Bax and promoting cytochrome *c* release and caspase-3 activation in the absence of any other upstream events. Alternatively, in the same cells Zn induced in a p53-independent manner expression of nuclear Bax gene resulting in elevated levels of cytosolic Bax (Feng et al. 2008, 2002). Conversely, p53 is clearly required for death signaling in MCF-7 breast cells where Zn-mediated apoptosis involved also oxidative stress and mitochondrial translocation of Bax (Ostrakhovitch and Cherian 2005). Similar mechanisms may be involved in ovarian cancer demise too as demonstrated in OVCAR-3 cells where Zn inhibited mitochondrial m-aconitase, increased Bax/Bcl-2 ratio and activated caspase-3 (Bae et al. 2006). In pancreatic adenocarcinoma cells PaCa44, CFPAC1, Panc1, and T3M4, Zn induced oxidative stress and translocation of apoptosis-inducing factor (AIF) into the nucleus, with resulting caspase-independent apoptosis (Donadelli et al. 2009). Oxidative stress as well as activation of extrinsic apoptosis via Fas was reported in Zn-treated murine mammary carcinoma cells (Provinciali et al. 2002). In addition, Zn-induced apoptosis of hepatoma cells H-7 required c-myc (Xu et al. 1996) while in Zn-exposed leukemic cells HL-60 p38 kinase was activated (Kondoh et al. 2002). Zn has also been reported to induce apoptosis in Jurkat T cells and Ramos B cells via increased expression of Bim and activation of caspases (Mann and Fraker 2005). Despite the fact that Zn has been shown to induce apoptosis, other types of cell death; i.e. necrosis or autophagy were associated with Zn exposure too (Iitaka et al. 2001). Still more importantly, regardless of cell type and particular cell death signals involved available evidence suggests mitochondria and recently lysosomes as important cellular compartments playing a significant role in initiation of the Zn-induced final cell death process (Feng et al. 2002; Lee et al. 2009).

In our previous work we showed that externally supplied Zn is capable of inducing apoptosis in human cervical cancer cells Hep-2 via mitochondria and oxidative stress (Rudolf et al. 2005). Nevertheless, the exact nature of Zn-induced upstream events preceding mitochondrial apoptosis was not clear. In addition, some of our unpublished previous observations indicated the involvement of lysosomes in Zn-mediated Hep-2 cell injury but its extent and potential crosstalk with mitochondria remained unresolved. Thus in this work we wanted to explore in detail Zn-induced stress signaling along with Zn-specific trafficking preceding Hep-2 cell death. We report that treatment of Hep-2 cells with zinc pyrithione (ZnPyr) leads to an early appearance of cytoplasmic Zn-specific foci with corresponding accumulation of Zn first in mitochondria and later in lysosomes. Concomitant with these changes, upregulation of expression of metallothionein II A gene (MT-IIA) as well as increased abundance of its protein occurs. Moreover, zinc activates p53 and its dependent genes including Puma and Bax and they contribute to an observed loss of mitochondrial membrane potential (MMP) and activation of apoptosis. Conversely, lysosomal membrane permeabilization and its promoted cleavage of Bid occurs at later treatment intervals with a limited effect on observed MMP loss. Finally, the use of specific inhibitors as well as siRNA technology suggest a crucial role of MT-IIA in trafficking of free Zn into mitochondria or lysosomes and regulation of apoptotic or necrotic cell demise.

Materials and methods

Cell line

Human cervical tumor cell line Hep-2 (ECACC, No. 86030501, Porton Down, UK) was cultivated in Dulbecco's modified Eagle's medium (DMEM, Gibco, Czech Republic), supplemented with 10% bovine serum (Gibco, Czech Republic), 100 U/ml penicillin, and 100 μg/ml streptomycin. The cells were maintained in plastic tissue-culture dishes (Nunclon, Denmark) in an incubator with 5% CO_2 at 37°C and passaged twice a week with 0.5% trypsin. Only mycoplasma-free cultures were used for experiments.

Chemicals

Zinc pyrithione (ZnPyr), *N*-acetylcysteine (NAC); 2′, 7′- Dichlorofluorescein diacetate (DCFH/DA), Zinquin ethyl ester, *N*,*N*,*N*′,*N*′- tetrakis(2-pyridylmethyl)ethylenediamine (TPEN), Acridine orange, coenzyme Q, 4′, 6-diamidino-2-phenylindole (DAPI), 3-[(3-cholamidopropyl)dimethylammonio]-1-propanesulfonic acid (CHAPS), dithiotreitol (DTT), dimethylsulfoxide (DMSO), propidium iodide and *β*-actin were purchased from Sigma–Aldrich (Prague, Czech Republic). JC-1; FluoZin-3 AM, RhodZin-3 AM and Trizol were from Invitrogen (Carlsbad, USA). WST-1 (4-[3-(4-iodophenyl)-2-(4-nitrophenyl)-2H-5-tetrazolio]-1,3-benzene disulfonate) was purchased from Boehringer Mannheim-Roche (Mannheim, Germany). Primary antibodies against cathepsin D, Bax, Puma, Ser-15 and Ser-46 phospho-p53 and p53 were purchased from Cell Signaling Technology, Inc. (Danvers, MA, USA). Primary antibody against cleaved Bid and metallothionein IIA were from Santa Cruz, Inc. (Santa Cruz, USA). Secondary antibodies were from Alexis Corporation (Lausen, Switzerland). p53-specific inhibitor Pifithrin and cathepsin D-specific inhibitor z-Phe-Gly-NHO-Bzz-VAD-fmk were acquired from Calbiochem (EMD Biosciences, Inc., La Jolla, CA, USA). All other chemicals were of highest analytical grade.

Cell treatments

ZnPyr was dissolved in DMSO to the final stock concentration of 1 mM. The working concentrations of ZnPyr were obtained by diluting the stock solution in treatment medium. The inhibitors and modulators were dissolved in either DMSO or serum-free medium as stock solutions. The working concentrations of individual chemicals were achieved by diluting their stock solutions in treatment medium and were as follows: NAC—antioxidant (1 mM—added to cells 24 h prior to ZnPyr exposure), Pifithrin—specific p53 inhibitor (30 μM—added to cells 1 h before ZnPyr exposure), coenzyme Q—membrane stabilizer (10 μM—added to cells concurrently with ZnPyr) and z-Phe-Gly-NHO-Bzz-VAD-fmk—specific inhibitor of cathepsin D (20 μM—supplemented to cells 30 min before addition of ZnPyr). Control cultures were treated with either the same dose of inhibitor or a corresponding volume of vehicle.

Cell proliferation

WST-1 is a colorimetric assay, which is based on the cleavage of the tetrazolium salt to colored formazan by mitochondrial dehydrogenases in viable cells. This assay quantifies cell proliferation and viability by measuring activity of mitochondrial enzymes and was for this reason used. Hep-2 cells at a concentration of 30,000 cells/well in 200 μl of DMEM containing 10% bovine serum were seeded in 96-well microtiter plates, with the first column of wells without cells (blank). The cells were allowed overnight at 37°C and in 5% CO_2. Next, cultures were exposed to ZnPyr and at various time points, medium with ZnPyr was aspirated, cultures were rinsed with PBS and 100 μl of WST-1 was added. The cells were further incubated for 2 h. The absorbance was recorded at 490 nm with 650 nm of reference wavelength by a scanning multiwell spectrophotometer (TECAN SpectraFluor Plus (TECAN Austria GmbH, Grödig, Austria)). In all cases, the absorbance of the tested substance in medium alone was recorded to determine whether it interfered with the assay. Each tested solution was tested in 16 independent wells.

Time-lapse videomicroscopy

Hep-2 cells were seeded into plastic tissue-culture dishes with glass bottom and left for 24 h in an incubator with 5% CO_2 at 37°C. Next day the growth medium was replaced with a medium containing different concentrations of ZnPyr. The tissue-culture

dishes were transferred into a time-lapse imaging system BioStation IM (Nikon, Prague, Czech Republic) combining an incubator, a motorized microscope and a cooled CCD camera. Recording was carried out in a multipoint and multichannel manner employing various time-lapse modes and upon small as well as high magnifications to allow global as well as detailed view of changes in behavior of treated cell populations. Recorded sequences were subsequently semi automatically analyzed with the software NIS Elements AR 2.30 (Nikon, Prague, Czech Republic).

Apoptosis assay

For determination of apoptosis, control and ZnPyr-treated Hep-2 cells grown n cultivation flasks were harvested with 0.1% trypsin, rinsed with PBS (5 min) and fixed in 70% ethanol at 4°C for 24 h. After rinsing fixed cells in PBS (5 min), cells were resuspended in a solution containing 0.1% Triton X-100, 50 μg/ml RNaseA and 0.5 μg/ml propidium iodide. Following the incubation (30 min, 25°C, dark), the apoptotic cell populations were determined using a flow cytometer Cell Lab Quanta™ SC (Beckman Coulter Inc. Brea, CA, USA). In addition, for independent verification of apoptosis, both control and ZnPyr-treated cells were harvested, washed with cold PBS (5 min), fixed with cold methanol (15 min, 25°C) and labeled with DAPI (10 μg/ml, 15 min, 25°C). Mounted specimens were examined under a fluorescence microscope Nikon Eclipse E 400 (Nikon, Prague, Czech Republic) (excitation filter 330–380 nm and emission filter 420 nm) equipped with a digital color matrix camera COOL 1300 (VDS, Vosskűhler, Germany). Photographs were taken using the software NIS Elements AR 2.30 and nuclei of at least 1,000 cells were quantified with subsequent morphometric analysis.

Criteria for determination of type of cell death

Cells were considered apoptotic when at least two independent proapoptotic markers were present; i.e. membrane blebbing (video microscopy), DNA content (flow cytometry), nuclear fragmentation (fluorescence microscopy) and caspase activation (caspase assays).

Necrotic cells were identified by rapid swelling in the absence of membrane blebbing, vacuolization (video microscopy), propidium iodide positivity (flow cytometry), random nuclear morphology (fluorescence microscopy) and low or absent caspase activity (caspase assays).

Fluorescent visualization of free Zn

Hep-2 cells were seeded plastic tissue-culture dishes with glass bottom and allowed to grow overnight at 37°C. After treatment with ZnPyr, cells in dishes were rinsed in PBS and stained with Zinquin (5 μM, 30 min, 37°C) or RhodZin–3 AM (3 μM, 30 min, 37°C). Following rinsing with warm cultivation medium the amount and distribution of free Zn (Zinquin) and free Zn in mitochondria (RhodZin–3 AM) in individual cells were assessed by a time-lapse imaging system BioStation IM (Nikon, Prague, Czech Republic) with subsequent analysis by the software NIS Elements AR 2.30 (Nikon, Prague, Czech Republic).

Fluorescent colocalization studies

Hep-2 cells were seeded into plastic tissue-culture dishes with glass bottom and left for 24 h in an incubator with 5% CO_2 at 37°C. Next day cells were transduced with Organelle Lights™ Mito-GFP and Organelle Lights™ Lysosomes-RFP kits (Invitrogen, Carlsbad, USA) to transiently label mitochondria and lysosomes according to manufacturer's protocol. Twenty-four hours post transduction, the efficiency of procedure was verified by fluorescence microscopy and specimens containing more than 60% positively labeled cells were exposed to ZnPyr. At individual time intervals, treated cells were stained with Zinquin (blue) or RhodZin–3 AM (red–orange) as described in previous section and colocalization of organelle-specific fluorescence signals (mitochondria—green and lysosomes—red) and free Zn-specific signals were monitored in a time-lapse imaging system BioStation IM (Nikon, Prague, Czech Republic). At each time interval, Z-stacks of at least 100 individual cells were generated with subsequent analysis of overlapping signals to determine a degree of colocalization with the software NIS Elements AR 2.30 (Nikon, Prague, Czech Republic).

Measurement of free intracellular Zn

Hep-2 cells were seeded in 96-well black walled plates and allowed to grow overnight in an incubator with 5% CO_2 at 37°C. At individual time intervals, 1 μM FluoZin-3 AM was added to both treated and control cells for 30 min. The fluorescence was measured using a multiplate reader TECAN SpectraFluor Plus (TECAN Austria GmbH, Grödig, Austria) at 520 nm. Free Zn concentrations in control and ZnPyr-treated cells were acquired using Grynkiewicz equation (Grynkiewicz et al. 1985). The fluorescence maxima were obtained with 50 μM ZnPyr and minima using 50 μM TPEN.

Measurement of total intracellular Zn

Treated and control Hep-2 cultures were harvested using trypsin (0.25% trypsin, Sigma–Aldrich, Prague, Czech Republic) and rinsed three times with cold phosphate buffered saline (PBS), with each rinsing followed by centrifugation for 5 min at 1,500 rpm (JOUAN MR 22, Trigon, Prague, Czech Republic) at room temperature (RT). The cells were dissolved in 0.35 ml 0.8% nitric acid and assayed for total Zn by atomic absorption with an inductively coupled plasma emission spectrometer MSD 5972 (Agilent Technologies, Waldbronn, Germany). Aliquots of cell samples prior to analysis were assayed for protein content using bicinchoninic acid assay—BCA assay (Bicinchoninic acid kit for protein determination, Sigma–Aldrich, Prague, Czech Republic).

Measurement of oxidative stress

Generation of hydrogen peroxide and/or hydroxyl radical was monitored by intracellular conversion of DFCH/DA into a fluorescent product dichlorofluorescein (DCF) (Ubezio and Civoli 1994). Hep-2 cells were seeded into cultivation flasks and cultivated to 80% confluence at 37°C. After exposure to ZnPyr, control and treated cells were detached by 0.1% trypsin and collected by centrifugation (50*g*, 5 min, 4°C—JOUAN M21, France). Next, the cells were resuspended in DMEM (pH adjusted to 7.2) and 5 μM DFCH/DA was added (5 min, 37°C). Changes in the fluorescence intensity (485 nm excitation; 538 nm emission) were measured by Shimadzu UV–Visible Spectrophotometer UV—1601 (SHIMADZU DEUTSCHLAND GmbH, Germany). The data were expressed as a percentage of fluorescence intensity increase per 10^6 cells.

Mitochondrial membrane potential

Hep-2 cells were seeded to 96-well plates with black bottom and allowed to grow overnight at 37°C and 5% CO_2. At specified time intervals following the treatment with ZnPyr, cells were rinsed in PBS and stained with cationic JC-1 dye (10 μg/ml) for 15 min at 37°C. Following the rinsing with warm cultivation medium, changes in mitochondrial membrane potential in at least 50,000 target cells for total assay were assessed by a multiplate reader TECAN SpectraFluor Plus (TECAN Austria GmbH, Grödig, Austria) at 485/520 nm (for the monomer form) and 520/590 nm (for the aggregate form) filter combinations, respectively. Results were expressed as percentage of control after blank subtraction.

Caspase activity

ZnPyr-treated and control cultures at 6, 12, 18 and 24 h were harvested by centrifugation (600 g, 5 min, JOUAN MR 22, Trigon, Prague, Czech Republic) and lysed on ice for 20 min in a lysis buffer containing 50 mM HEPES, 5 mM CHAPS and 5 mM DTT. The lysates were centrifuged at 14,000*g*, 10 min, 4°C, and the supernatants were collected and stored at −80°C. The enzyme activity was measured in a 96-well microplate using a kinetic fluorometric method based on the hydrolysis of the fluorogenic caspase-specific substrate (DEVD-AFC for caspase-3, Ac-LEHD-AFC for caspase-9, IETD-AFC for caspase-8 VDVAD-AFC for caspase-2 and Ac-DEVD-pNA for caspase-7, 37°C, 1 h) by individual caspases. Specific inhibitors of caspase-9, -8, -2, -3 and -7 were used to confirm the specificity of the cleavage reaction. Fluorescence was recorded at 460/40 nm after excitation at 360/40 nm using TECAN SpectraFluor Plus (TECAN Austria GmbH, Grödig, Austria). Results are shown as fold increase in activity relative to untreated cells.

Real-time PCR

Total RNA was isolated from ZnPyr-treated cells at 0, 3, 6, 12 and 16 h with Trizol. RNA was resuspended

in RNAse-free water, digested with DNAse I and purified using Qiagen columns (Qiagen, Hideer, Germany). The quality and quantity of obtained RNA was verified by UV–Vis spectrophotometry. Real-time RT-PCR was performed with the High pure PCR template preparation kit (Roche, Prague, Czech Repulic) according to the manufacturer's protocol using LightCycler 1.5 (Roche, Prague, Czech Repulic). cDNA was amplified in total 50 cycles with the following conditions: 30 s denaturation at 95°C (30 s), annealing at 60°C (30 s) and extension at 70°C (35 s). MTIIa primer sequences were as follows: forward primer AAGTCCCAGCGAACCCGCGT and reverse primer CAGCAGCTGCACTTGTCCGA CGC. Obtained melting curves indicated no primer-dimer formation. β-actin was used as an internal control for each reaction to ensure equal loading of RNA. Created amplification plots and the threshold cycle were used to calculate the fold change of MT-IIA gene.

Gene knockdown

Hep-2 cells were seeded into six well culture plates in antibiotic-free DMEM with 10% BS and kept in an incubator upon 37°C and 5% CO_2 to reach 60–70% confluence. Knockdown of MT-IIA and Bid were carried out using siRNAs transfection kits from Santa Cruz Biotechnology, Inc. (Santa Cruz, USA) and knockdown of Bax was achieved by the SignalSilence® Pool Bax siRNA (Cell Signaling Technology) following the manufacturer's protocol. The cells were exposed to ZnPyr and analyzed 36 h after the last siRNA transfection.

Cell lysates

ZnPyr-treated and control cells were harvested at different time intervals with trypsin, washed with PBS and centrifuged (2000 rpm, 5 min, 4°C). The resulting pellet was used for preparation of whole cell lysates; cells were resuspended in 5 ml of ice-cold lysis buffer (137 mM NaCl, 10% glycerol, 1% *n*-octyl-β-D-glucopyranoside, 50 mM NaF, 20 mM Tris, 1 mM sodium orthovanadate and Complete TMMini) and stored at −20°C until further use.

Immunobloting

The whole cell lysates were boiled for 5 min/95°C in SDS sample buffer (Tris–HCl pH 6.81, 2-mercaptoethanol, 10% glycerol, SDS, 0.1% bromphenol blue) and thereafter they were loaded onto a 12% SDS/polyacrylamide gel. Each lysate contained equal amount of protein (30 μg) as determined by BCA assay (bicinchoninic acid—Sigma, Prague, Czech Republic). After electrophoresis, proteins were transferred to a PVDF membrane (100 V, 60 min) and incubated at 25°C for 1.5 h with a solution containing 5% nonfat dry milk, 10 mM Tris–HCl (pH 8.0), 150 mM sodium chloride, and 0.1% Tween 20 (TBST). Membranes were incubated with primary antibodies (anti-Bax, 1:600; anti Puma, 1:1000; anti-p53, 1:450; anti-p-p53 (Ser-15), 1:300; anti-p-p53 (Ser-46), 1:500; anti-cathepsin D, 1:250; anti-cleaved Bid, 1.500 and anti-β-actin, 1:750) at 4°C overnight followed by five 6 min washes in TBST. Next, the blots were incubated with secondary peroxidase-conjugated antibodies (1:1,000, 1 h, 25°C), washed with TBST and the signal was developed with a chemiluminescence (ECL) detection kit (Boehringer Mannheim-Roche, Basel, Switzerland). Protein loading was correlated to β-actin expression.

Lysosomal membrane assay

Control and ZnPyr-treated Hep-2 cells at individual treatment intervals were stained with 5 μM acridine orange for 15 min. After rinsing them twice with fresh incubation medium, acridine orange redistribution was measured fluorimetrically using a SpectraFluorPlus (TECAN Austria GmbH, Grödig, Austria) spectrofluorimeter at 490 nm excitation and 530 emission wavelengths. Lysosomal membrane damage was expressed as an increase in diffuse cytosolic green fluorescence by acridine orange released from lysosomes (Pourahmad et al. 2001).

Statistics

Statistical analysis was carried out with a statistical program GraphPad Prism 4.0 (GraphPad Software, Inc. San Diego, USA) with one-way Anova test and Dunnett's post test for multiple comparisons. Results

were compared with control samples, and means were considered significant if $P < 0.05$.

Results

Dose-dependent effects of zinc pyrithione on Hep-2 cell proliferation and apoptosis

The effects of ZnPyr on Hep-2 cells proliferation and apoptosis were examined with the WST-1 assay and flow cytometric determination of apoptotic cells during 24 h of treatment. Figure 1a shows dose-dependent cytotoxicity of ZnPyr which first became significant at the concentration of 500 nM but the extent of observed inhibitory effect did not change at higher employed doses. Conversely, significantly elevated apoptosis in ZnPyr-treated Hep-2 cells was detected already at 50 nM concentration, however, the peak apoptotic response was reached with 500 nM and 1 μM concentrations and at higher doses the levels of apoptosis in treated Hep-2 cells decreased (Fig. 1b). Corresponding studies with pyrithione showed that its effect in the same concentration range and time frame on Hep-2 cells apoptosis was insignificant (data not shown). Time-lapse video microscopy as well as fluorescence studies confirmed these findings, in particular specific morphological changes in treated cells; i.e. cell shrinkage, loss of adherence, membrane blebbing and specific chromatin fragmentation in ZnPyr-treated cells (Fig. 1c, d). Since the maximum apoptosis was induced by 500 nM ZnPyr which also was the lowest tested dose to significantly inhibit proliferation of Hep-2 cells, this concentration was used in further experiments.

Zinc pyrithione elevates intracellular free Zn and targets it into various compartments

Intracellular free Zn concentrations in Hep-2 cells treated with 500 nM ZnPyr during 24 h were determined by Zn-specific probes Zinquin (microscopy) and FluoZin-3 AM (microfluorimetry). Fluorescence microscopy revealed an increasing intensity of fluorescence in treated cells already between 6 and 8 h of exposure, respectively. This intensity rapidly grew and reached the peak between 14 and 16 h of treatment, with no further change till the end of experiment. Zn-specific fluorescence signals first appeared in the form of tiny oscillating speckles scattered throughout the cytoplasm of cells with gradual grouping and clumping of speckles into cluster-like structures (Fig. 2a). Quantitative measurements showed that the initial 0.5 nM free Zn concentration increased during first 14 h of treatment with ZnPyr almost four times to 1.86 nM whereas total intracellular Zn concentration grew from 230 to 280 μM in the same treatment interval (Fig. 2b).

To determine whether observed punctuate Zn-specific fluorescence signals reflect its random cytoplasmic distribution or specific subcellular compartment localization, we transduced cells with baculovirus directing specific autofluorescence proteins into mitochondria (GFP-green) and lysosomes (RFP-red) and compared their distribution with the one visualized by Zinquin. Kinetics of topography of individual signals and their subsequent analysis revealed that significant colocalization of free Zn with lysosomes occurred at the end of treatment only (24 h). Conversely, free Zn colocalized with mitochondria already at 12 h of exposure (Fig. 3a, b). To verify Zn-specific distribution in mitochondria we next employed Zn-indicator RhodZin-3 which effectively detects changes of intramitochondrial free Zn concentrations (Sensi et al. 2003a, b). As shown in Fig. 3c, ZnPyr at 500 nM concentration markedly increased intramitochondrial free Zn concentrations as early as at 6 h of treatment and by 12 h intramitochondrial pools of free Zn were massively elevated.

Zinc pyrithione-induced apoptosis requires mitochondria with limited involvement of lysosomes

Since we found that upon treatment of Hep-2 cells with ZnPyr a rapid and significant accumulation of free Zn in mitochondria and to some extent in lysosomes occurs, we wanted to investigate a potential contribution of these organelles to observed apoptosis. We first measured mitochondrial membrane potential (MMP) of exposed cells and discovered that from 12 h of treatment it significantly decreased (Fig. 4a). This decrease corresponded to kinetics of cytochrome *c* release (data not shown), elevated activities of caspase-9, caspase-3 and caspase-7. On the other hand, the activity of caspase -2 remained relatively low and activity of caspase-8

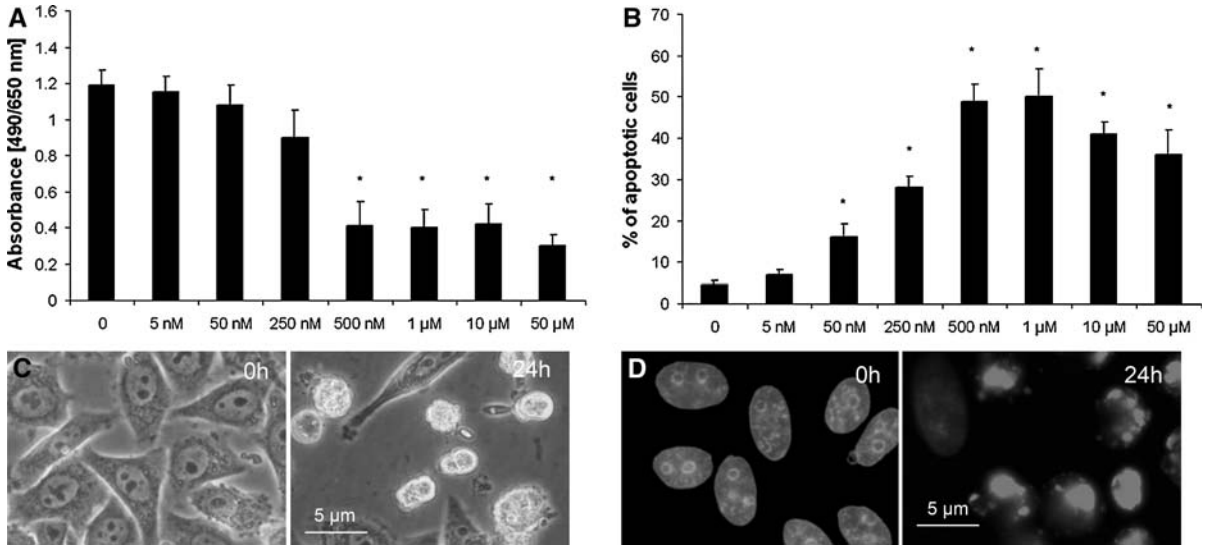

Fig. 1 Dose dependent effects of zinc pyrithione (ZnPyr) on proliferation as measured by WST-1 colorimetric assay (**a**) and apoptosis as determined by flow cytometry, time-lapse videomicroscopy (phase contrast, magnification ×600) and fluorescence microscopy (magnification ×600) (**b**, **c** and **d**) of Hep-2 tumor cells during 24 h of exposure. Cells were treated with a range of ZnPyr concentrations and individual endpoints were analyzed as described in "Materials and methods" section. Images are representative of at least three independent experiments and show morphology of Hep-2 cells and their nuclei at the beginning and at the end of treatment. Other results represent means ± SD of at least three experiments * $P < 0.05$ compared to untreated control cells with one way-Anova test and Dunnett's post test for multiple comparisons

markedly increased only at later treatment intervals (18–24 h) (Fig. 4b). Collapse of lysosomal membrane integrity and subsequent proteases-mediated cleavage of Bid are postulated mechanisms leading to apoptosis (Guicciardi et al. 2004). We used lysosomal membrane damage assay which quantifies the extent of acridine orange displacement from lysosomes to the cytoplasm. The results of this assay show that in 500 nM ZnPyr exposed Hep-2 cells the translocation of acridine orange into cytoplasm occurred at late treatment intervals (Fig. 4c). In addition, Western blot analysis of the expression of a lysosomal enzyme cathepsin D and cleavage of Bid in treated Hep-2 cells indicated similar time profile, with marked increases in expression of both markers occurring at the end of treatment (Fig. 4d).

Zinc pyrithione-induced MMP decrease depends on p53-pathway and metallothionein IIA presence but occurs independently of oxidative stress

There are various factors and mechanisms which may decrease MMP and induce permeability transition with the activation of mitochondrial apoptosis in treated cells. Concerning acknowledged intracellular targets of Zn, we firstly focused on oxidative stress. Treatment of Hep-2 cells with 500 nM ZnPyr resulted in gradually increasing levels of reactive oxygen species (ROS) whose abundance nevertheless did not become significant until the end of experiment (Fig. 5a). To verify whether increased free Zn stimulates antioxidant response in exposed cells we measured the expression of MT-IIA, a known Zn-inducible antioxidant. Figure 5b shows an early upregulation of MT-IIA gene expression in ZnPyr-treated cells, with the maximum transcription activity being at 6 h of treatment. On the other hand, the corresponding protein levels significantly increased during en entire experiment and reached the maximum at the end of treatment. Next, we examined whether increased intracellular free Zn interacted with DNA and, in particular with p53. Our data show that 500 nM ZnPyr increased expression of p53 which also became significantly phosphorylated at Ser-15 and Ser-46. Moreover, the increased expression of p53 coincided with elevated levels of Bax and Puma too albeit at longer treatment period (12 h) (Fig. 5c). To determine the effect of individual analyzed markers on the observed decrease in MMP, we employed pharmacological inhibitors of

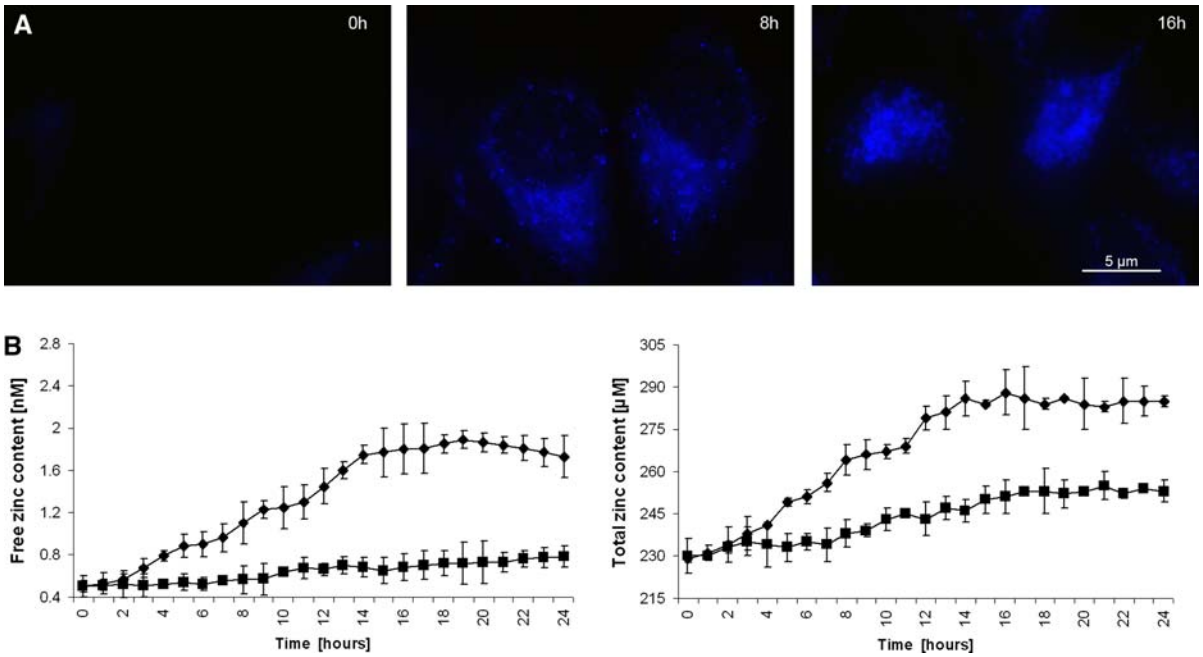

Fig. 2 Effects of 500 nM zinc pyrithione (ZnPyr) on free and total intracellular zinc levels as measured by free zinc-specific fluorescent probes Zinquin (5 µM, microscopy) and Fluo-Zin3-AM (1 µM, microfluorimetry) as well as by atomic absorption spectrometry in Hep-2 cervical tumor cells during 24 h of exposure. **a** Treated cells loaded with Zinquin were at regular time intervals visualized by fluorescent microscopy at ×600 magnification and images were captured with the NIS Elements AR 2.30 software as described in "Materials and methods" section. Images represent three experiments **b** Kinetics of changes in free zinc concentrations (Fluo-Zin3-AM) and total zinc concentrations (absorption spectrometry) were determined as described in "Materials and methods" section. Results represent means ± SD of at least three independent experiments

oxidative stress (NAC), p53 (Pifithrin) as well as specifically suppressed the expression of Bax, Bid and MT-IIA using siRNA technology. The data presented in Fig. 5d indicate that the inhibition of p53 as well as Bax and MT-IIA significantly prevented 500 nM ZnPyr-induced decrease in MMP in Hep-2 cells while blocking of oxidative stress with NAC and knockdown of Bid failed to do so. In addition, the best protection was observed in MT-IIA knockdown cells where despite the presence of ZnPyr MMP was almost completely restored.

Prevention of free Zn localization into mitochondria increases free Zn accumulation in lysosomes and leads to necrosis

To gain further insight into the role of MT-IIA in sequestering free Zn in treated Hep-2 cells, we monitored free Zn specific fluorescence in MT-IIA knockdown cells both in mitochondria and lysosomes. We found that in cells with suppressed expression of MT-IIA free Zn-specific fluorescence developed more rapidly and intensively but with significantly lower targeted accumulation in mitochondria (Fig. 6a, b). By contrast, colocalization of free Zn and lysosomes was markedly increased as early as at 6 h of treatment. Also, lysosomal membrane integrity was significantly altered, resulting in massive acridine orange translocation and increased presence of cathepsin D in the cytoplasm (Fig. 6c, d). Morphologically, cells underwent rapid development of extensive cytoplasmic vacuolization followed by swelling, shrinkage and fragmentation which are consistent with reported observations of necrotic cell death. Inhibition of lysosomal disruption with coenzyme Q and inhibition of cathepsin D with the specific inhibitor z-Phe-Gly-NHO-Bzz-VAD-fmk attenuated the entire process and delayed cell death

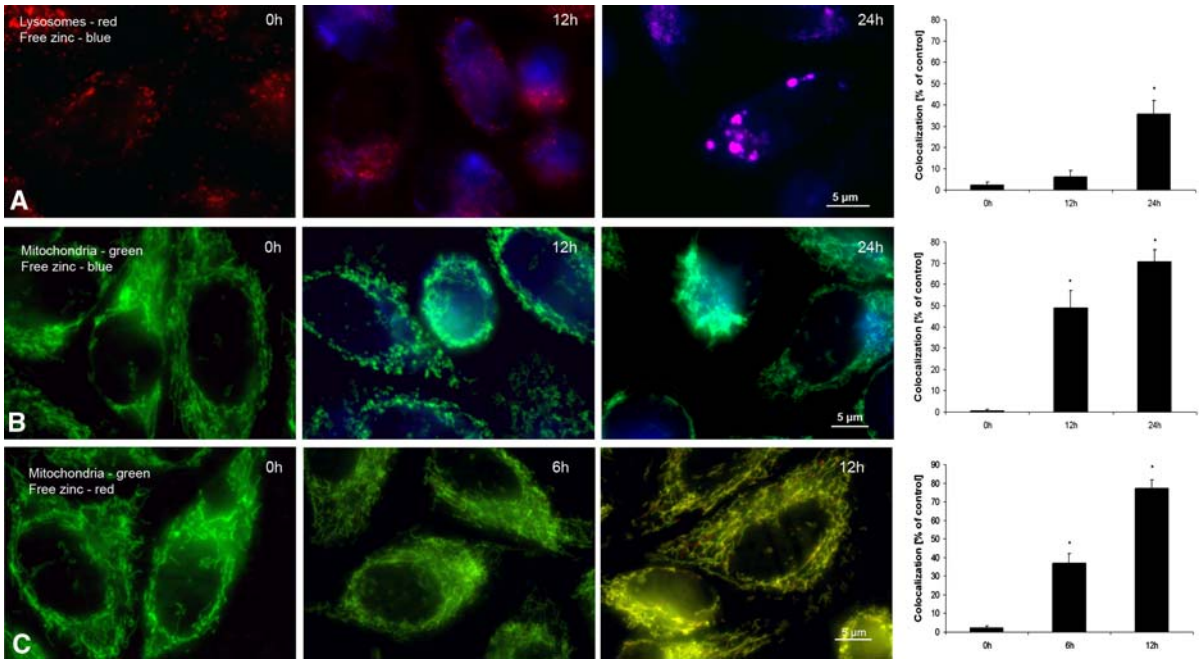

Fig. 3 Intracellular distribution and localization of free zinc in 500 nM zinc pyrithione (ZnPyr) treated Hep-2 tumor cells during 24 h of exposure. **a** Intracellular localization of free zinc (Zinquin-blue) and its time-dependent colocalization with lysosomes (RFP-labeled) **b** Intracellular localization of free zinc (Zinquin-blue) and its time-dependent colocalization with mitochondria (GFP-labeled) cells **c** Intracellular localization of free zinc in mitochondria (RhodZin–3 AM-red) and its time-dependent colocalization with mitochondria (GFP-labeled). The nature of fluorescence signal distribution and colocalization was followed at ×600 magnification and quantifications were carried out with the NIS Elements AR 2.30 software as described in "Materials and methods" section. Images are representative of at least tree independent experiments. Colocalization results represent means ± SD of at least three experiments. * $P < 0.05$ compared to the beginning of treatment with one way-Anova test and Dunnett's post test for multiple comparisons

which morphologically exhibited features of apoptosis rather then necrosis (Fig. 6e–g).

Discussion

Increases in intracellular free Zn are associated with an acute cellular injury and subsequent cell death in both normal as well as tumor cells. Previous studies suggested that cellular targets of elevated intracellular free Zn are diverse and may include organelles such as mitochondria or lysosomes, particular enzymatic systems or individual nuclear genes (Dineley et al. 2003; Kindermann et al. 2005; Ostrakhovitch and Cherian 2005; Yu et al. 2009). Moreover, available evidence in the literature suggests differing dynamics of this process in various models, with relative scarcity of data in solid tumor cells (Ostrakhovitch and Cherian 2004). In the present study we chose solid tumor cell line Hep-2 derived from cervical cancer mainly due to its sensitivity to zinc supplementation and well characterized stress responses including excellent morphological as well as molecular characteristics of cell death (Rudolf et al. 2005). We used ZnPyr to directly increase intracellular free Zn levels and to observe dynamics of the cell response to this treatment. This chemical was shown before to induce apoptosis in murine thymocytes as well as human leukemia cells via increased expression of Bim but its activity in solid tumor cells remains unclear (Mann and Fraker 2005).

The results from the present study demonstrate dose-dependent antiproliferative and proapoptotic effects of ZnPyr which are directly related to observable increased intracellular free Zn levels. Acquired baseline levels of free and total intracellular Zn in Hep-2 cells correspond to the previously published concentrations in human adenocarcinoma HT-29 cells (Krezel and Maret 2006). Moreover, kinetics of free Zn elevation in Hep-2 cells exposed

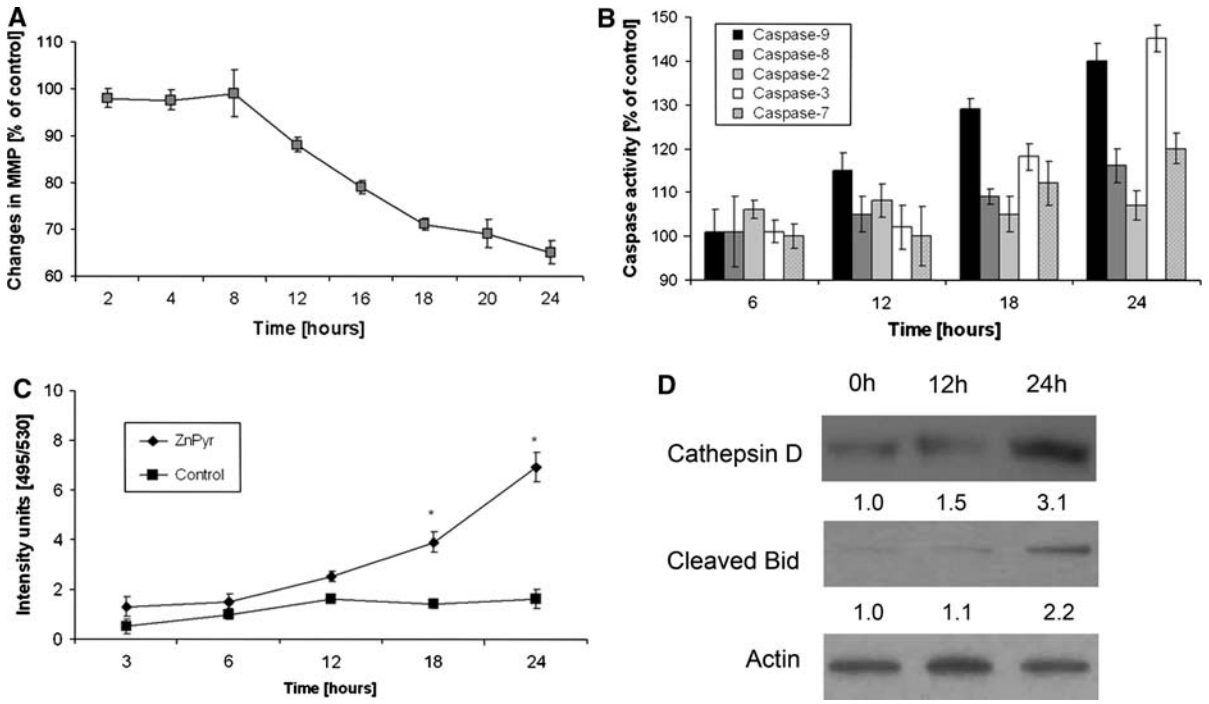

Fig. 4 Effects of 500 nM zinc pyrithione (ZnPyr) on **a** mitochondrial membrane potential (MMP) **b** caspase activities **c** lysosomal membrane disruption **d** and cathepsin D and Bid expression in tumor Hep-2 cells during 24 h. MMP was determined by microfluorimetric measurement of potential-sensitive JC-1 dye. Kinetics of caspase activities were measured by colorimetry-based enzyme-substrate reaction. Lysosomal membrane integrity was quantitated via colorimetric determination of acridine orange translocation from lysosomes into the cytoplasm. Cathepsin D expression and appearance of cleaved Bid in treated cells were quantified by immunoblotting with β-actin expression used to correct protein loading and with subsequent band analysis with GelQuant Ver 2.7 software (DNR Bio-Imaging Systems, Jerusalem, Israel) as described in "Materials and methods" section. Results represent means $\pm$ SD of at least three experiments * $P < 0.05$ compared to untreated control cells with one way-Anova test and Dunnett's post test for multiple comparisons

to ZnPyr reflects on some aspects of free Zn buffering capacity of Hep-2 cells with contribution of induced MT-IIA. In addition, observed changes in free and total intracellular Zn concentrations after treatment with ZnPyr for the first time demonstrate the extent of this change and make it possible to link this it with subsequent biological effects in cervical cancer cells. Detailed cytometric analyses of treated Hep-2 cells revealed punctuate free Zn-specific fluorescence signals in the form of oscillating foci whose dynamics and subcellular localization suggested their non-random pattern of distribution. Using fluorescent protein-labeled mitochondria and lysosomes we found increased early colocalization of free Zn with mitochondria, with this finding further confirmed by free Zn-specific intramitochondrial probe Rhodzin-3. On the other hand, lysosomes did not accumulate free Zn until late periods of treatment and this observation was again confirmed by a delayed loss of lysosomal membrane integrity, slowly increasing expression of cathepsin D and generation of a cleaved Bid. Moreover, ZnPyr-induced apoptosis as verified by specific morphology of Hep-2 cells (cell shrinkage and detachment and membrane blebbing), early loss of MMP and activation of caspases did involve mitochondria but the contribution of lysosomes was in this case very limited. This finding thus confirms mitochondria as a crucial target of free Zn activity in cervical tumor Hep-2 cells and supports similar observations in other solid tumor cell lines (Feng et al. 2002; Ostrakhovitch and Cherian 2005). Still, elevated free Zn may preferentially interact with lysosomes and induce apoptosis via cleavage of Bid as was shown in prostate cancer cells treated with clioquinol (Yu et al. 2009). This differential intracellular targeting of free Zn thus seems to depend on

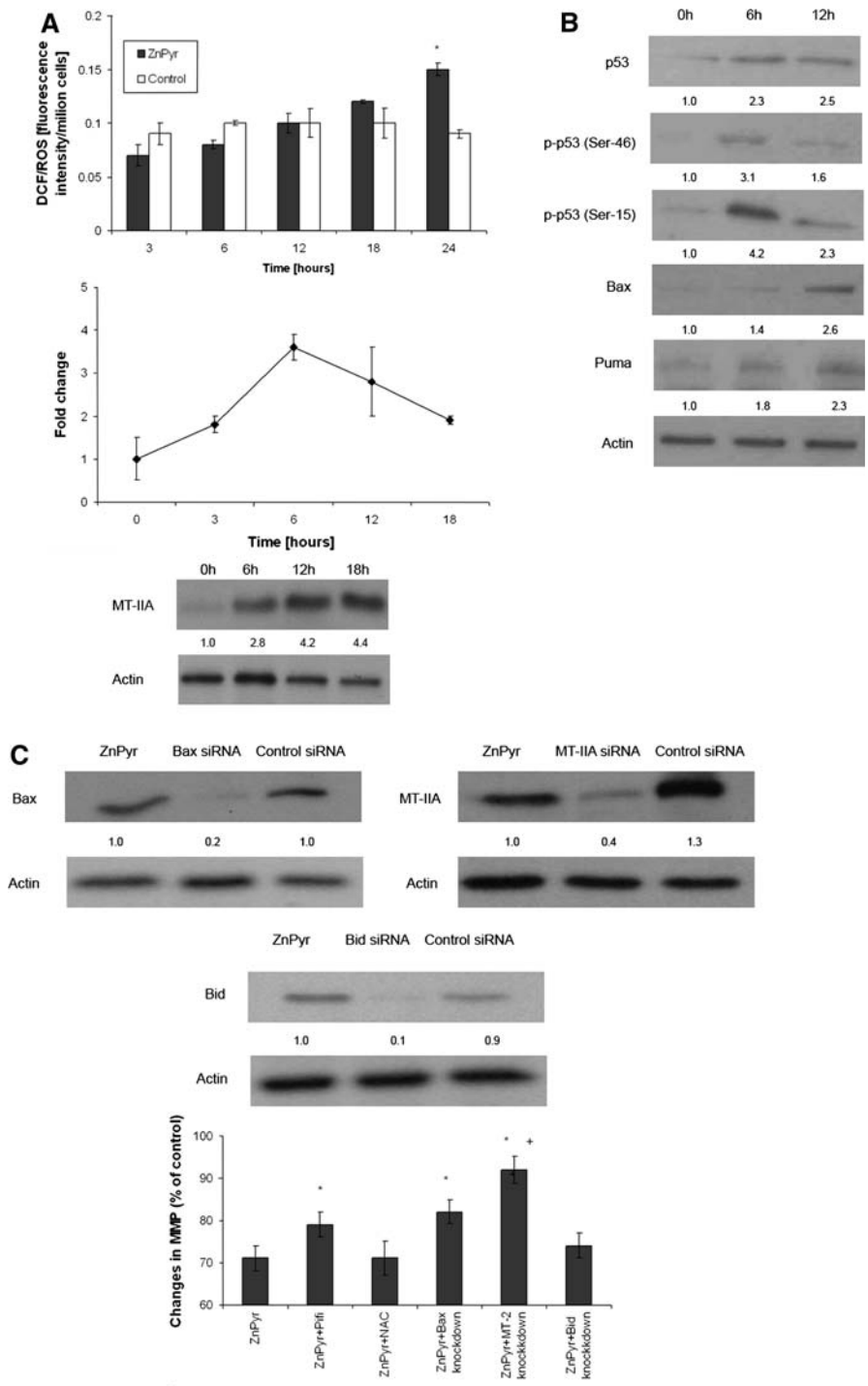

cell type as well as the nature of free Zn generation. On the whole, differences in free Zn originating from different sources following diverse stresses and its preferential intracellular trafficking may prove to be important not only for our understanding of Zn biology but also for the potential use of free Zn elevating chemicals in treatment of cancer. Since a considerable part of research concerning proapoptotic

◀**Fig. 5** **a** Oxidative stress and the expression of metallothionein IIA (MT-IIA) in tumor Hep-2 cells treated with 500 nM zinc pyrithione (ZnPyr) during 24 h. Oxidative stress was determined spectrophotometrically by intracellular conversion of 2′-7′-dichlorodihydrofluorescein diacetate (DFCH/DA) into a fluorescent product dichlorofluorescein (DCF). Kinetics of expression of metallothonein IIA (MT-IIA) was carried out with real-time PCR and immunoblotting analysis as described in "Materials and methods" section. β-actin expression used to correct protein loading and relative quantifications of protein expression were measured using GelQuant Ver 2.7 software (DNR Bio-Imaging Systems, Jerusalem, Israel). Results represent means ± SD of at least three experiments. * $P < 0.05$ compared to control cultures with one way-Anova test and Dunnett's post test for multiple comparisons. **b** Expression and activation of p53 and p53-dependent genes Bax and Puma in 500 nM zinc pyrithione (ZnPyr)-treated tumor Hep-2 cells during 24 h. Cells were lysed and protein expression was determined by immunoblotting with β-actin expression used to correct protein loading and with subsequent band analysis with GelQuant Ver 2.7 software (DNR Bio-Imaging Systems, Jerusalem, Israel) as described in "Materials and methods" section. Shown are representative images representing at least three experiments. **c** Effects of pharmacological inhibition as well as specific knockdown technology on 500 nM zinc pyrithione (ZnPyr)-induced decrease in mitochondrial membrane potential (MMP) in tumor Hep-2 cells during 24 h of treatment. Cells were pretreated with oxidative stress-inhibiting *N*-acetyl cystein (NAC) and the specific p53 inhibitor Pifithrin prior to ZnPyr exposure and changes in MMP were determined as described in "Materials and methods" section. Alternatively, prior to ZnPyr treatment Bax, metallothionein IIA (MT-IIA) and Bid expressions were reduced with the specific siRNA and changes in MMP were determined as described in "Materials and methods" section. Images show efficiency of siRNA against Bax, Bid and MT-IIA protein expression in at least three experiments. Other results represent means ± SD of at least three experiments. * $P < 0.05$ compared to ZnPyr treated cells and $+P < 0.05$ compared to Pifithrin-treated cells or cells with inhibited Bax expression with one way-Anova test and Dunnett's post test for multiple comparisons

role of zinc in cancer cells is focused on prostate gland which has a rather unique position due to its specificity of Zn metabolism, verification of Zn-specific effects on mitochondria, lysosomes or other compartments and molecules in different cancer cell lines is necessary to prove general validity of experimental findings.

Thus besides aforementioned targets, increased free Zn levels have been reported to be genotoxic via generation of oxidative stress or via specific DNA binding (Ostrakhovitch and Cherian 2005; Provinciali et al. 2002). Still, our data do not indicate significant involvement of oxidative stress in ZnPyr-treated Hep-2 cells. One explanation of this controversy may be the upregulation of antioxidant systems in exposed cells. Zn has been shown to induce expression of reduced glutathione (Cortese et al. 2008) and/or of metallothioneins—small cysteine-rich proteins which belong among biological systems in eukaryotic cells with proposed antioxidant function (Davis and Cousins 2000). Concerning our previous studies (Rudolf 2007), we focused on MT-IIA and found its early but transient upregulation in ZnPyr-treated cells. On the other hand, the corresponding MT-IIA protein expression increased with time, thereby indicating possible elevated stability of this protein which is also likely to explain moderate buildup of ROS levels in exposed cells. In parallel with these changes, we found an increased expression and specific phosphorylation of p53 protein in treated Hep-2 cells along with increased abundance of Bax and Puma proteins. p53 and its target gene Bax have already been reported as important targets of Zn toxicity and apoptosis in breast and prostate cancer cells (Feng et al. 2008; Ostrakhovitch and Cherian 2005) but our data about the specific free Zn-mediated p53 phosphorylation and simultaneous activation of Bax and Puma are novel and significantly extend our understanding of this interaction and its involvement in apoptosis. To this end, it is interesting to note that Zn was able to induce p53-dependent response in Hep-2 cells but in the absence of significant caspase-2 activation which has been shown to be characteristic of DNA-damage response observed after several cytostatics (Zhivotovsky and Orrenius 2005). The most likely explanation here is the nature of interaction between Zn and DNA molecules as well as the final extent of DNA damage which is clearly much less extensive and special in case of Zn than in case of DNA-damaging cytostatics.

Loss of MMP is understood as a prerequisite for the triggering of the executionary phase of apoptosis. Due to the fact that ZnPyr-treated Hep-2 cells exhibited an early decrease in MMP, next we wanted to investigate into the mechanism of this phenomenon. We employed specific pharmacological inhibitors while suppressing the expression of MT-IIA, Bax and Bid genes using siRNA technology. Predictably, both suppression of p53 as well as knockdown of Bax attenuated ZnPyr-mediated decrease in MMP of Hep-2 cells while antioxidant NAC and knockdown of Bid showed no effect in this respect. Surprisingly,

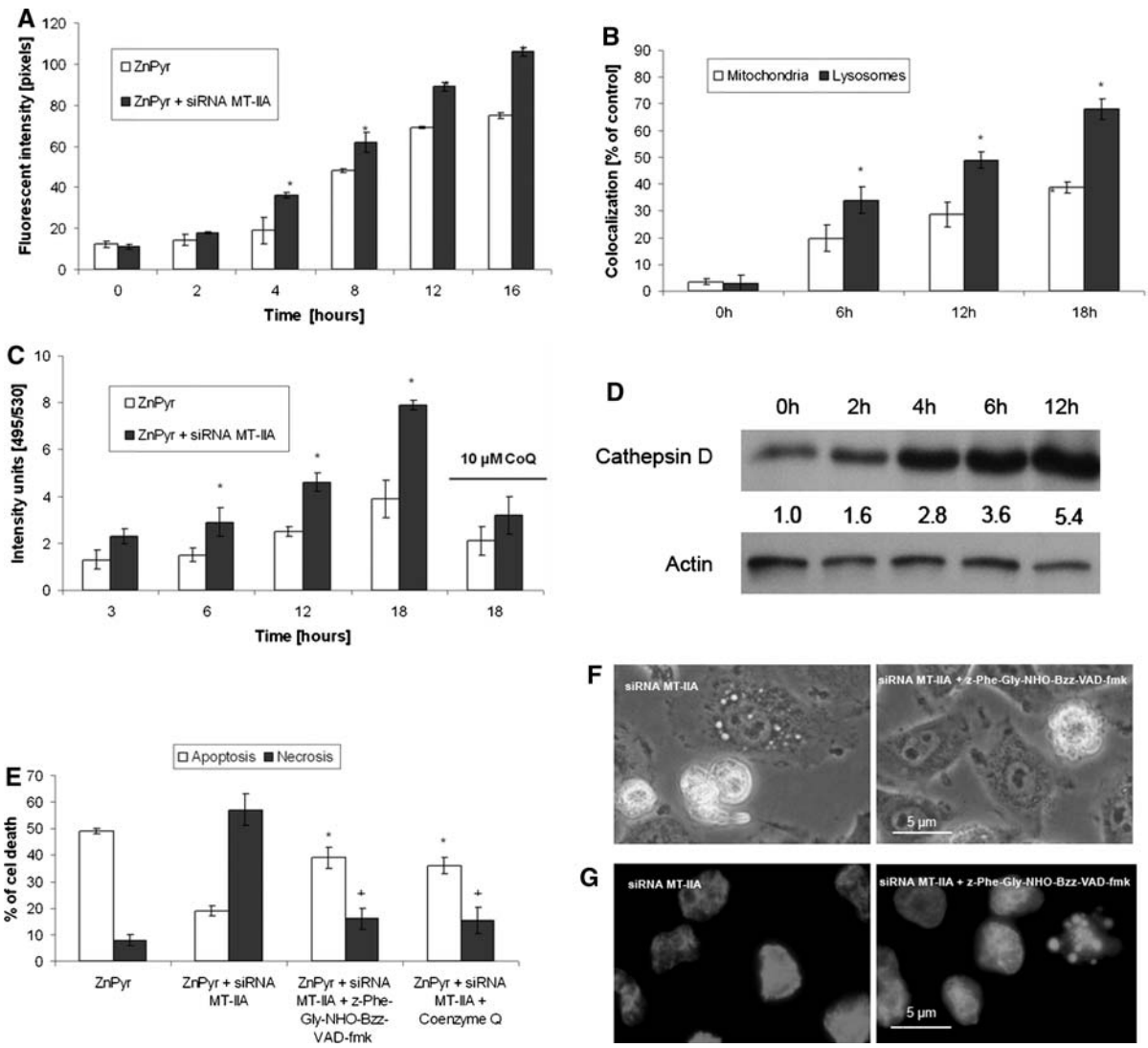

knockdown of MT-IIA almost completely restored loss of MMP in ZnPyr treated Hep-2 cells, suggesting the special involvement of this molecule in Zn-mitochondria interaction. Metallothioneins have been suggested as putative transporters of Zn into mitochondria (Ye et al. 2001). Furthermore, an increased expression of metallothioneins was proposed to lead to enhanced presence of free Zn levels in the cell by the conditional release of bound Zn ions (Maret and Vallee 1998). Our data agree with these hypotheses as ZnPyr exposed Hep-2 cells with MT-IIA knockdown accumulated higher free Zn levels and, importantly, free Zn localized in lysosomes rather than in mitochondria. Thus it appears that in the present model MT-IIA serves as a free Zn sequestering molecule which may on one hand transport Zn into mitochondria while recycling it to keep intracellular free Zn at high levels. The nature of Zn transport into mitochondria remains unresolved; however, as the results of specific studies suggest other potential transport mechanisms such as calcium-specific uniporters (Malaiyandi et al. 2005). Whether these uniporters, metallothioneins or other as yet unidentified transport means are involved in specific mitochondrial trafficking of Zn requires further investigation. The other important finding from our experiments points at the fact that in the absence of functional MT-IIA elevated free Zn levels target lysosomes, which in turn leads to their disruption and increased expression of cathepsin D. In addition, in

◀ **Fig. 6** **a**, **b** Effects of metallothionein II A (MT-IIA) knock down on 500 nM zinc pyrithione (ZnPyr)-induced free zinc accumulation (**a**) and localization in mitochondria (**b**) in tumor Hep-2 cells during 24 h treatment. Fluorescence signals representing free-zinc levels and their colocalization with GFP-labeled mitochondria or RFP-labeled lysosomes were quantified and analyzed using the NIS Elements AR 2.30 software as described in "Materials and methods" section. Results represent means ± SD of at least three experiments. * $P < 0.05$ compared to ZnPyr treated cells with one way-Anova test and Dunnett's post test for multiple comparisons. **c**, **d** Effects of metallothionein II A (MT-IIA) knockdown on 500 nM zinc pyrithione (ZnPyr)-induced lysosomal disruption (**c**) and cathepsin D expression (**d**) in Hep-2 cells during 24 h treatment. Lysosomal membrane integrity was measured via colorimetric determination of acridine orange translocation from lysosomes into the cytoplasm, with membrane stabilizing coenzyme Q significantly reducing ZnPyr-induced lysosomal membrane disruption. Cathepsin D expression was quantified by immunoblotting with subsequent band analysis with GelQuant Ver 2.7 software (DNR Bio-Imaging Systems, Jerusalem, Israel) as described in "Materials and methods" section. Protein loading was normalized to β-actin levels. Immunoblots represent results of at least three experiments. The other results represent means ± SD of at least three experiments. * $P < 0.05$ compared to ZnPyr treated cells with one way-Anova test and Dunnett's post test for multiple comparisons. **e**, **f** Effects of pharmacological inhibition as well as specific knock down technology on 500 nM zinc pyrithione (ZnPyr)-induced cell death in tumor Hep-2 cells during 24 h of treatment. Cells with downregulated metallothionein IIA (MT-IIA) gene expression were pretreated with cathepsin D inhibitor z-Phe-Gly-NHO-Bzz-VAD-fmk or the membrane stabilizing coenzyme Q prior to ZnPyr exposure and cell death mode was determined via flow cytometry, video microscopy (phase contrast, ×600 magnification) and fluorescence microscopy (magnification ×600) as described in "Materials and methods" section. Images show morphologies of siRNA MT-IIA Hep-2 cells with typical cytoplasmic vacuoles, irregular cellular swelling and nuclear architecture typical of necrosis (12 h) as well as apoptotic cell blebbing and nuclear condensation in the same cells pretreated with cathepsin D inhibiting z-Phe-Gly-NHO-Bzz-VAD-fmk (12 h). Other results represent means ± SD of at least three experiments. * $P < 0.05$ compared to apoptosis rate in ZnPyr-treated MT-IIA knock down cells and $+P < 0.05$ compared to necrosis rate in ZnPyr-treated MT-IIA knock down cells with one way-Anova test and Dunnett's post test for multiple comparisons

thus dysfunctional cells extensive cytoplasmic vacuolization develops and the prevailing type of cell death is observed necrosis. When either lysosomal disruption is blocked with membrane stabilizing coenzyme Q or cathepsin D expression is reduced with the specific inhibitor z-Phe-Gly-NHO-Bzz-VAD-fmk, apoptotic phenotype is restored in treated cells and cell death becomes slightly delayed too.

Cell death-specific communication between mitochondria and lysosomes has been explored in the past although details about involved mechanisms are by far not completely elucidated (Kim 2005). Despite the fact that elevated intracellular free Zn is known to be capable of inducing apoptosis or necrosis in various cells via either mitochondria or lysosomes the crosstalk of both compartments in Zn mediated cell death has not been reported so far. Our findings suggest that at least in the present model mitochondria represent primary target of free Zn which via induced expression of MT-IIA may enter and act to decrease MMP along with p53 upregulated Bax and Puma. Lysosomes here seem to play only a supportive role, acting as a possible amplifier via cleavage of Bid and its translocation into mitochondria to promote MMP loss. Nevertheless, upon absence of functional MT-IIA, free Zn massively enters lysosomes, induces their disruption leading to increased expression of cathepsin D with subsequent rapid necrotic cell demise. Thus MT-IIA acts as master regulator of free intracellular Zn localization as well as of cell death modality in Hep-2 cervical tumor cells.

Acknowledgments This work was supported by Ministry of Education of Czech Republic Research Project MSM 0021620820.

References

Bae SN, Lee YS, Kim MY, Kim JD, Park LO (2006) Antiproliferative and apoptotic effects of zinc-citrate compound (CIZAR(R)) on human epithelial ovarian cancer cell line, OVCAR-3. Gynecol Oncol 103:127–136

Cortese MM, Suschek CV, Wetzel W, Kroncke KD, Kolb-Bachofen V (2008) Zinc protects endothelial cells from hydrogen peroxide via Nrf2-dependent stimulation of glutathione biosynthesis. Free Radic Biol Med 44:2002–2012

Davis SR, Cousins RJ (2000) Metallothionein expression in animals: a physiological perspective on function. J Nutr 130:1085–1088

Dineley KE, Votyakova TV, Reynolds IJ (2003) Zinc inhibition of cellular energy production: implications for mitochondria and neurodegeneration. J Neurochem 85:563–570

Donadelli M, Dalla Pozza E, Scupoli MT, Costanzo C, Scarpa A, Palmieri M (2009) Intracellular zinc increase inhibits p53(-/-) pancreatic adenocarcinoma cell growth by ROS/AIF-mediated apoptosis. Biochim Biophys Acta 1793:273–280

Feng P, Li TL, Guan ZX, Franklin RB, Costello LC (2002) Direct effect of zinc on mitochondrial apoptogenesis in prostate cells. Prostate 52:311–318

Feng P, Li T, Guan Z, Franklin RB, Costello LC (2008) The involvement of Bax in zinc-induced mitochondrial apoptogenesis in malignant prostate cells. Mol Cancer 7:25

Franklin RB, Costello LC (2007) Zinc as an anti-tumor agent in prostate cancer and in other cancers. Arch Biochem Biophys 463:211–217

Grynkiewicz G, Poenie M, Tsien RY (1985) A new generation of Ca2 + indicators with greatly improved fluorescence properties. J Biol Chem 260:3440–3450

Guicciardi ME, Leist M, Gores GJ (2004) Lysosomes in cell death. Oncogene 23:2881–2890

Hogstrand C, Verbost PM, Wendelaar Bonga SE (1999) Inhibition of human erythrocyte Ca2 + -ATPase by Zn2+. Toxicology 133:139–145

Iitaka M, Kakinuma S, Fujimaki S, Oosuga I, Fujita T, Yamanaka K, Wada S, Katayama S (2001) Induction of apoptosis and necrosis by zinc in human thyroid cancer cell lines. J Endocrinol 169:417–424

Kim R (2005) Recent advances in understanding the cell death pathways activated by anticancer therapy. Cancer 103: 1551–1560

Kindermann B, Doring F, Fuchs D, Pfaffl MW, Daniel H (2005) Effects of increased cellular zinc levels on gene and protein expression in HT-29 cells. Biometals 18:243–253

Kondoh M, Tasaki E, Araragi S, Takiguchi M, Higashimoto M, Watanabe Y, Sato M (2002) Requirement of caspase and p38MAPK activation in zinc-induced apoptosis in human leukemia HL-60 cells. Eur J Biochem 269:6204–6211

Krezel A, Maret W (2006) Zinc-buffering capacity of a eukaryotic cell at physiological pZn. J Biol Inorg Chem 11:1049–1062

Lee SJ, Cho KS, Koh JY (2009) Oxidative injury triggers autophagy in astrocytes: the role of endogenous zinc. Glia 57:1351–1361

Malaiyandi LM, Vergun O, Dineley KE, Reynolds IJ (2005) Direct visualization of mitochondrial zinc accumulation reveals uniporter-dependent and -independent transport mechanisms. J Neurochem 93:1242–1250

Mann JJ, Fraker PJ (2005) Zinc pyrithione induces apoptosis and increases expression of Bim. Apoptosis 10:369–379

Maret W (2009) Molecular aspects of human cellular zinc homeostasis: redox control of zinc potentials and zinc signals. Biometals 22:149–157

Maret W, Vallee BL (1998) Thiolate ligands in metallothionein confer redox activity on zinc clusters. Proc Natl Acad Sci USA 95:3478–3482

Maret W, Jacob C, Vallee BL, Fischer EH (1999) Inhibitory sites in enzymes: zinc removal and reactivation by thionein. Proc Natl Acad Sci USA 96:1936–1940

Ostrakhovitch EA, Cherian MG (2004) Differential regulation of signal transduction pathways in wild type and mutated p53 breast cancer epithelial cells by copper and zinc. Arch Biochem Biophys 423:351–361

Ostrakhovitch EA, Cherian MG (2005) Role of p53 and reactive oxygen species in apoptotic response to copper and zinc in epithelial breast cancer cells. Apoptosis 10:111–121

Pourahmad J, Ross S, O_Brien PJ (2001) Lysosomal involvement in hepatocyte cytotoxicity induced by Cu(2 +) but not Cd(2 +). Free Radic Biol Med 30:89–97

Provinciali M, Donnini A, Argentati K, Di Stasio G, Bartozzi B, Bernardini G (2002) Reactive oxygen species modulate Zn(2 +)-induced apoptosis in cancer cells. Free Radic Biol Med 32:431–445

Rudolf E (2007) Depletion of ATP and oxidative stress underlie zinc-induced cell injury. Acta Medica (Hradec Kralove) 50:43–49

Rudolf E, Rudolf K, Cervinka M (2005) Zinc induced apoptosis in HEP-2 cancer cells: the role of oxidative stress and mitochondria. Biofactors 23:107–120

Sensi S, Jeng J (2004) Rethinking the excitotoxic ionic milieu: the emerging role of Zn(2 +) in ischemic neuronal injury. Curr Mol Med 4:87–111

Sensi S, Ton-That D, Sullivan P, Jonas E, Gee K, Kaczmarek L, Weiss J (2003a) Modulation of mitochondrial function by endogenous Zn2 + pools. Proc Natl Acad Sci USA 100:6157–6162

Sensi S, Ton-That D, Weiss J, Rothe A, Gee K (2003b) A new mitochondrial fluorescent zinc sensor. Cell Calcium 34:281–284

Ubezio P, Civoli F (1994) Flow cytometric detection of hydrogen peroxide production induced by doxorubicin in cancer cells. Free Radic Biol Med 16:509–516

Xu J, Xu Y, Nguyen Q, Novikoff PM, Czaja MJ (1996) Induction of hepatoma cell apoptosis by c-myc requires zinc and occurs in the absence of DNA fragmentation. Am J Physiol 270:G60–G70

Ye B, Maret W, Vallee BL (2001) Zinc metallothionein imported into liver mitochondria modulates respiration. Proc Natl Acad Sci USA 98:2317–2322

Yu H, Zhou Y, Lind SE, Ding WQ (2009) Clioquinol targets zinc to lysosomes in human cancer cells. Biochem J 417:133–139

Zhivotovsky B, Orrenius S (2005) Caspase-2 function in response to DNA damage. Biochem Biophys Res Commun 331:859–867